J. Fluid Mech. (1994), *vol.* 268, *pp.* 133–145

Analogy between laminar flows in curved pipes and orthogonally rotating pipes

By HIROSHI ISHIGAKI

Kakuda Research Center, National Aerospace Laboratory, Kakuda, Miyagi, Japan

(Received 19 October 1992 and in revised form 19 November 1993)

The secondary flow of a viscous fluid, caused by the Coriolis force, through a straight pipe rotating about an axis perpendicular to the pipe axis is analogous to that of a fluid, caused by the centrifugal force, through a stationary curved pipe. The quantitative analogy between these two fully developed laminar flows will be demonstrated through similarity arguments, computational studies and the use of experimental data. Similarity considerations result in two analogous governing parameters for each flow, which include a new one for the rotating flow. When one of these analogous pairs of parameters of the two flows is large, it will be demonstrated that there are strong similarities between the two flows regarding friction factors, heat transfer rates, flow patterns and flow properties for the same values of the other pair of parameters.

1. Introduction

The study of viscous flow in stationary curved ducts is of fundamental interest in fluid mechanics. When a viscous fluid flows through a curved pipe, a cross-stream pressure gradient is balanced by a centrifugal force in the rapidly flowing central core of the flow, while the slower flowing fluid along the walls of the pipe is forced inward where the pressure is less. A secondary flow then takes place perpendicular to the main flow. The resulting double spiral flow increases pressure loss and heat transfer rate significantly.

There are many examples of curved pipe flows in engineering applications and in nature. They can be found in piping systems, flow passages of turbomachinery, coils in heat exchangers and in blood flow. The first major theoretical advance on laminar flow in a curved pipe was made by Dean (1927, 1928), who showed that fully developed laminar flow in slightly curved pipes depends primarily on a single dimensionless parameter, now called the Dean number. Since then, numerous studies have been made on this topic theoretically, experimentally and computationally. Computational studies on fully developed laminar flows have been made by McConalogue & Srivastava (1968), Truesdell & Adler (1970), Akiyama & Cheng (1971), Austin & Seader (1973), Patanker, Pratap & Spalding (1974), Collins & Dennis (1975), Dennis & Ng (1982), Nandakumar & Masliyah (1982) and Soh & Berger (1987). Studies on curved pipe flow have been extensively surveyed by Berger, Talbot & Yao (1983), Nandakumar & Masliyah (1986) and Ito (1987).

Another example of secondary flow, caused by the Coriolis force, occurs when viscous fluids flow through a straight pipe which is rotating about an axis perpendicular to the pipe axis. Such rotating passages are used in the cooling systems for rotor blades of gas turbines as well as other flow passages in rotating machinery. The patterns of this secondary flow are similar to those observed in secondary flow through a stationary curved pipe.

Theoretical studies on laminar flows in orthogonally rotating pipes have been made by Barua (1954), Benton & Boyer (1966), Mori & Nakayama (1968) and Ito & Nanbu (1971). Ito & Nanbu (1971) also conducted experiments for a wide range of parameters and provided experimental formulae on the friction factor. Computational studies have been made on pipe flow by Skiadaressis & Spalding (1977), Ito, Hasegawa & Yano (1986), Lei & Hsu (1990) and Ishigaki & Tamura (1990), and on square duct flow by Speziale (1982), Kheshgi & Scriven (1985) and Komiyama, Mikami & Okui (1986). Studies on rotating pipe flow up to 1980 are summarized in Morris (1981).

It has sometimes been noted in previous studies that there is an analogy between flow through stationary curved pipes and flow through orthogonally rotating straight pipes, in the sense that the longitudinal curvature plays a role similar to that of orthogonal rotation. This analogy has, however, been described in purely qualitative terms. Thangam & Hur (1990), for example, mentioned this analogy in the appendix of their paper on secondary flow in curved rectangular ducts. They noted that the Rossby number in rotating duct flow corresponds with the curvature ratio in curved duct flow. But they gave neither a dimensionless number that corresponds with the Dean number (a fundamental parameter in curved duct flow) nor any quantitative results. We know of no studies on the quantitative similarities between these two flows. In this study we will show that there is a strong quantitative analogy between fully developed laminar flows in curved pipes and orthogonally rotating pipes.

In order to discuss similarities or show an analogy between two different kinds of flow, it is essential to use proper similarity parameters (dimensionless numbers). It is well known that the dynamical similarity for steady laminar flow in curved pipes depends on two dimensionless parameters: the Dean number $K_{LC} = Re/\lambda^{\frac{1}{2}}$ and the curvature ratio $\lambda = R/d$ (see Berger *et al.* 1983). In the above definitions d denotes the diameter of the pipe, R the mean radius of curvature of the pipe, and Re the flow Reynolds number $w_m d/\nu$, where w_m represents the mean velocity of flow through the pipe and ν the fluid kinematic viscosity. This combination has an important property in that the flow characteristics become independent of λ when the λ is large enough, so they depend only on the Dean number. We call this property an 'asymptotic invariance property' of the second parameter.

For laminar flow in an orthogonally rotating pipe, various combinations of parameters have been used to correlate the flow characteristics. Barua (1954) used Re and the rotation number, which is the inverse of the Rossby number $Ro = w_m/\Omega d$, where Ω is the angular velocity of rotation. Ito & Nanbu (1971) used $K_l = ReR_\Omega$ and the rotational Reynolds number $R_\Omega = \Omega d^2/\nu$, while Lei & Hsu (1990) used $R_\Omega G$ and R_Ω^2 where G denotes the Reynolds number based on the axial pressure gradient. Kheshgi & Scriven (1985) used R_Ω and Ro while Speziale (1982) used Re and Ro. However, none of these sets correspond with K_{LC} and λ in curved pipe flow, so they do not have the 'asymptotic invariance property'. In this paper we will introduce a new dimensionless parameter $K_{LR} = Re/Ro^{\frac{1}{2}}$, which was first used by Ishigaki & Tamura (1990) to correlate their computational results. We will take K_{LR} and the Rossby number Ro as a set corresponding to K_{LC} and λ in curved pipe flow.

When λ and Ro are large enough in their respective flows, K_{LC} and K_{LR} are the sole parameters that determine the dynamical behaviour of each flow. This study will demonstrate that, when λ and Ro are large, the friction factors and heat transfer rates for these two flows coincide when $K_{LC} = K_{LR}$. It will also be shown that the variations of the flow properties, such as the maximum secondary velocity, with K_{LC} or K_{LR} are very similar.

In the next section we will discuss similarity parameters and proper similarity

transformations for each flow, and then show that these sets of parameters actually have an asymptotic invariance property of λ and Ro when they are large. This will be followed by discussions of the computational results concerning friction factors, heat transfer rates, flow patterns and flow properties in axial and cross-stream directions.

2. Formulation and dimensionless parameters

2.1. *Flow in curved pipes*

Although similarity parameters have been firmly established for curved pipe flow, here we will clarify the similarity transformation, the velocity and the length scales of this flow. The toroidal coordinates (r, θ, ϕ) will be used as shown in figure 1. The velocities in the directions of (r, θ, ϕ) are denoted by (u, v, w). It is assumed that the flow is incompressible steady laminar and fully developed. Since u, v and w are independent of ϕ in the fully developed region, the equations of continuity and motion are (e.g. Ward-Smith 1980)

$$\frac{1}{r}\frac{\partial}{\partial r}(ru)+\frac{1}{r}\frac{\partial v}{\partial \theta}+\frac{1}{R+r\cos\theta}(u\cos\theta-v\sin\theta)=0, \tag{1}$$

$$u\frac{\partial u}{\partial r}+\frac{v}{r}\frac{\partial u}{\partial \theta}-\frac{v^2}{r}-\frac{w^2\cos\theta}{R+r\cos\theta}=-\frac{1}{\rho}\frac{\partial p}{\partial r}+\nu\left[\nabla^2 u+\frac{\cos\theta}{R+r\cos\theta}\frac{\partial u}{\partial r}-\frac{\sin\theta}{r(R+r\cos\theta)}\frac{\partial u}{\partial \theta}\right.$$
$$\left.-\left(\frac{1}{r^2}+\frac{\cos^2\theta}{(R+r\cos\theta)^2}\right)u-\frac{2}{r^2}\frac{\partial v}{\partial \theta}+\frac{v\sin\theta}{R+r\cos\theta}\left(\frac{1}{r}+\frac{\cos\theta}{R+r\cos\theta}\right)\right], \tag{2}$$

$$u\frac{\partial v}{\partial r}+\frac{v}{r}\frac{\partial v}{\partial \theta}+\frac{uv}{r}+\frac{w^2\sin\theta}{R+r\cos\theta}=-\frac{1}{\rho r}\frac{\partial p}{\partial \theta}+\nu\left[\nabla^2 v+\frac{\cos\theta}{R+r\cos\theta}\frac{\partial v}{\partial r}-\frac{\sin\theta}{r(R+r\cos\theta)^2}\frac{\partial v}{\partial \theta}\right.$$
$$\left.-\left(\frac{1}{r^2}+\frac{\sin^2\theta}{(R+r\cos\theta)^2}\right)v+\frac{2}{r^2}\frac{\partial u}{\partial \theta}-\frac{R\sin\theta}{r(R+r\cos\theta)^2}u\right], \tag{3}$$

$$u\frac{\partial w}{\partial r}+\frac{v}{r}\frac{\partial w}{\partial \theta}+\frac{w}{R+r\cos\theta}(u\cos\theta-v\sin\theta)=-\frac{1}{\rho R}\frac{\partial p}{\partial \phi}+\nu\left[\nabla^2 w+\frac{\cos\theta}{R+r\cos\theta}\frac{\partial w}{\partial r}\right.$$
$$\left.-\frac{\sin\theta}{r(R+r\cos\theta)}\frac{\partial w}{\partial \theta}-\frac{w}{(R+r\cos\theta)^2}\right], \tag{4}$$

where p is the pressure and ρ the density. The Laplacian operator is

$$\nabla^2 \equiv \frac{\partial^2}{\partial r^2}+\frac{1}{r}\frac{\partial}{\partial r}+\frac{1}{r^2}\frac{\partial^2}{\partial \theta^2}.$$

In the fully developed region, it follows that

$$-\frac{1}{R}\frac{\partial p}{\partial \phi}=C_1, \tag{5}$$

where C_1 is a constant.

The velocity scale of the secondary flow, U_{SC}, will be obtained by retaining the inertia and centrifugal terms in (2) or (3) as

$$U_{SC}=w_m(d/R)^{\frac{1}{2}}=w_m/\lambda^{\frac{1}{2}}. \tag{6}$$

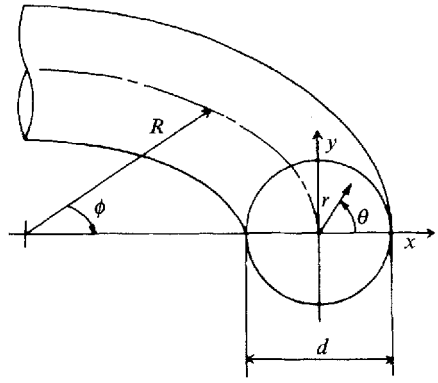

FIGURE 1. Configuration of curved pipe flow.

The cross-sectional quantities u, v and p will be scaled by U_{SC}, and the axial quantities w and C_1 by w_m. The scaled variables are

$$\tilde{u} = \frac{u}{w_m}\lambda^{\frac{1}{2}}, \quad \tilde{v} = \frac{v}{w_m}\lambda^{\frac{1}{2}}, \quad \tilde{w} = \frac{w}{w_m}, \quad \tilde{C}_1 = \frac{d\lambda^{\frac{1}{2}}}{\rho w_m^2} C_1, \quad \tilde{p} = \frac{p\lambda}{\rho w_m^2}, \quad \tilde{r} = \frac{r}{d}. \tag{7}$$

The dimensionless governing equations based on these variables are then given by

$$\frac{1}{\tilde{r}}\frac{\partial}{\partial \tilde{r}}(\tilde{r}\tilde{u}) + \frac{1}{\tilde{r}}\frac{\partial \tilde{v}}{\partial \theta} + \frac{1}{\lambda + \tilde{r}\cos\theta}(\tilde{u}\cos\theta - \tilde{v}\sin\theta) = 0, \tag{8}$$

$$\tilde{u}\frac{\partial \tilde{u}}{\partial \tilde{r}} + \frac{\tilde{v}}{\tilde{r}}\frac{\partial \tilde{u}}{\partial \theta} - \frac{\tilde{v}^2}{\tilde{r}} - \frac{\lambda \tilde{w}^2 \cos\theta}{\lambda + \tilde{r}\cos\theta} = -\frac{\partial \tilde{p}}{\partial \tilde{r}} + \frac{1}{K_{LC}}\left[\nabla^2 \tilde{u} + \frac{\cos\theta}{\lambda + \tilde{r}\cos\theta}\frac{\partial \tilde{u}}{\partial \tilde{r}} - \frac{\sin\theta}{\tilde{r}(\lambda + \tilde{r}\cos\theta)}\frac{\partial \tilde{u}}{\partial \theta}\right.$$
$$\left. - \left(\frac{1}{\tilde{r}^2} + \frac{\cos^2\theta}{(\lambda + \tilde{r}\cos\theta)^2}\right)\tilde{u} - \frac{2}{\tilde{r}^2}\frac{\partial \tilde{v}}{\partial \theta} + \frac{\tilde{v}\sin\theta}{\lambda + \tilde{r}\cos\theta}\left(\frac{1}{\tilde{r}} + \frac{\cos\theta}{\lambda + \tilde{r}\cos\theta}\right)\right], \tag{9}$$

$$\tilde{u}\frac{\partial \tilde{v}}{\partial \tilde{r}} + \frac{\tilde{v}}{\tilde{r}}\frac{\partial \tilde{v}}{\partial \theta} + \frac{\tilde{u}\tilde{v}}{\tilde{r}} + \frac{\lambda \tilde{w}^2 \sin\theta}{\lambda + \tilde{r}\cos\theta} = -\frac{1}{\tilde{r}}\frac{\partial \tilde{p}}{\partial \theta} + \frac{1}{K_{LC}}\left[\nabla^2 \tilde{v} + \frac{\cos\theta}{\lambda + \tilde{r}\cos\theta}\frac{\partial \tilde{v}}{\partial \theta} - \frac{\sin\theta}{\tilde{r}(\lambda + \tilde{r}\cos\theta)}\frac{\partial \tilde{v}}{\partial \theta}\right.$$
$$\left. - \left(\frac{1}{\tilde{r}^2} + \frac{\sin^2\theta}{(\lambda + \tilde{r}\cos\theta)^2}\right)\tilde{v} + \frac{2}{\tilde{r}^2}\frac{\partial \tilde{u}}{\partial \theta} - \frac{\lambda \tilde{u}\sin\theta}{\tilde{r}(\lambda + \tilde{r}\cos\theta)^2}\right], \tag{10}$$

$$\tilde{u}\frac{\partial \tilde{w}}{\partial \tilde{r}} + \frac{\tilde{v}}{\tilde{r}}\frac{\partial \tilde{w}}{\partial \theta} + \frac{\tilde{w}(\tilde{u}\cos\theta - \tilde{v}\sin\theta)}{\lambda + \tilde{r}\cos\theta} = \tilde{C}_1 + \frac{1}{K_{LC}}\left[\nabla^2 \tilde{w} + \frac{\cos\theta}{\lambda + \tilde{r}\cos\theta}\frac{\partial \tilde{w}}{\partial \tilde{r}}\right.$$
$$\left. - \frac{\sin\theta}{\tilde{r}(\lambda + \tilde{r}\cos\theta)}\frac{\partial \tilde{w}}{\partial \theta} - \frac{\tilde{w}}{(\lambda + \tilde{r}\cos\theta)^2}\right]. \tag{11}$$

Here, $K_{LC} = Re/\lambda^{\frac{1}{2}}$ is the Dean number, which is equal to the ratio of the square root of the product of inertia and centrifugal forces to the viscous force. This is a fundamental parameter in curved pipe flow and plays the same role as the Reynolds number for laminar flow in a stationary straight pipe. It is actually the Reynolds number based on the velocity scale U_{SC} and the lengthscale d in cross-section. The curvature ratio $\lambda = R/d$ denotes the ratio of the inertia force to the centrifugal force. From the above equations we can see that the two parameters, K_{LC} and λ, characterize laminar flow in curved pipes.

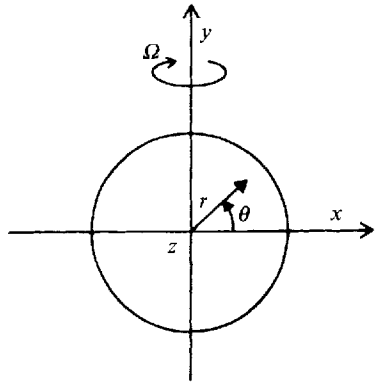

FIGURE 2. Configuration of an orthogonally rotating pipe flow.

If we bring λ to infinity, the limiting forms of (8)–(11) do not include λ, as shown in the following:

$$\frac{\partial}{\partial\tilde{r}}(\tilde{r}\tilde{u})+\frac{\partial\tilde{v}}{\partial\theta}=0, \tag{12}$$

$$\tilde{u}\frac{\partial\tilde{u}}{\partial\tilde{r}}+\frac{\tilde{v}}{\tilde{r}}\frac{\partial\tilde{u}}{\partial\theta}-\frac{\tilde{v}^2}{\tilde{r}}-\tilde{w}^2\cos\theta=-\frac{\partial\tilde{p}}{\partial\tilde{r}}+\frac{1}{K_{LC}}\left(\nabla^2\tilde{u}-\frac{\tilde{u}}{\tilde{r}^2}-\frac{2}{\tilde{r}^2}\frac{\partial\tilde{v}}{\partial\theta}\right), \tag{13}$$

$$\tilde{u}\frac{\partial\tilde{v}}{\partial\tilde{r}}+\frac{\tilde{v}}{\tilde{r}}\frac{\partial\tilde{v}}{\partial\theta}+\frac{\tilde{u}\tilde{v}}{\tilde{r}}+\tilde{w}^2\sin\theta=-\frac{1}{\tilde{r}}\frac{\partial\tilde{p}}{\partial\theta}+\frac{1}{K_{LC}}\left(\nabla^2\tilde{v}-\frac{\tilde{v}}{\tilde{r}^2}+\frac{2}{\tilde{r}^2}\frac{\partial\tilde{u}}{\partial\theta}\right), \tag{14}$$

$$\tilde{u}\frac{\partial\tilde{w}}{\partial\tilde{r}}+\frac{\tilde{v}}{\tilde{r}}\frac{\partial\tilde{w}}{\partial\theta}=\tilde{C}_1+\frac{1}{K_{LC}}\nabla^2\tilde{w}. \tag{15}$$

Flow characteristics are then independent of λ, and the flow system exhibits an asymptotic invariance property. As these 'loose coil' approximated equations of curved pipe flow are solved numerically in this study, the effects of λ are not included in the computational results. The experimental data on the friction factor (Ito 1959) and computational studies on the finite curvature effects (Austin & Sieder 1973; Soh & Berger 1987) show that the effects of λ are practically negligible when λ is larger than approximately 8.

2.2. *Flow in rotating pipes*

For flow in orthogonally rotating pipes, we will make formulations parallel to those for curved pipe flow and look for the dimensionless parameters that correspond to K_{LC} and λ. The cylindrical polar coordinates (r, θ, z) fixed to a rotating straight pipe will be used, as shown in figure 2. The pipe rotates about the y-axis at a constant angular velocity Ω. For fully developed laminar flow of incompressible fluids, the equations of continuity and motion are

$$\frac{\partial}{\partial r}(ru)+\frac{\partial v}{\partial\theta}=0, \tag{16}$$

$$u\frac{\partial u}{\partial r}+\frac{v}{r}\frac{\partial u}{\partial\theta}-\frac{v^2}{r}-2\Omega w\cos\theta=-\frac{1}{\rho}\frac{\partial p^*}{\partial r}+\nu\left(\nabla^2u-\frac{u}{r^2}-\frac{2}{r^2}\frac{\partial v}{\partial\theta}\right), \tag{17}$$

$$u\frac{\partial v}{\partial r}+\frac{v}{r}\frac{\partial v}{\partial\theta}+\frac{uv}{r}+2\Omega w\sin\theta=-\frac{1}{\rho r}\frac{\partial p^*}{\partial\theta}+\nu\left(\nabla^2v-\frac{v}{r^2}+\frac{2}{r^2}\frac{\partial u}{\partial\theta}\right), \tag{18}$$

$$u\frac{\partial w}{\partial r}+\frac{v}{r}\frac{\partial w}{\partial\theta}+2\Omega(u\cos\theta-v\sin\theta)=-\frac{1}{\rho}\frac{\partial p^*}{\partial z}+\nu\nabla^2w, \tag{19}$$

where p^* is the reduced pressure given by

$$p^* = p - \tfrac{1}{2}\rho\Omega^2(r^2\cos^2\theta + z^2). \tag{20}$$

As in the case of curved pipe flow, $\partial p^*/\partial z$ is constant,

$$-\frac{\partial p^*}{\partial z} = C_2. \tag{21}$$

By retaining the inertia and Coriolis terms in (17) or (18), the velocity scale of secondary flow in the rotating pipe is estimated to be

$$U_{SR} = (\Omega w_m d)^{\frac{1}{2}} = w_m/Ro^{\frac{1}{2}}. \tag{22}$$

The following transformations which are parallel to (7) will be made:

$$\tilde{u} = \frac{u}{w_m}Ro^{\frac{1}{2}}, \quad \tilde{v} = \frac{v}{w_m}Ro^{\frac{1}{2}}, \quad \tilde{w} = \frac{w}{w_m}, \quad \tilde{C}_2 = \frac{d\,Ro^{\frac{1}{2}}}{\rho w_m^2}C_2, \quad \tilde{p}^* = \frac{p^*Ro}{\rho w_m^2}, \quad \tilde{r} = \frac{r}{d}. \tag{23}$$

Scaled forms of (16)–(19) are

$$\frac{\partial}{\partial\tilde{r}}(\tilde{r}\tilde{u}) + \frac{\partial\tilde{v}}{\partial\theta} = 0, \tag{24}$$

$$\tilde{u}\frac{\partial\tilde{u}}{\partial\tilde{r}} + \frac{\tilde{v}}{\tilde{r}}\frac{\partial\tilde{u}}{\partial\theta} - \frac{\tilde{v}^2}{\tilde{r}} - 2\tilde{w}\cos\theta = -\frac{\partial\tilde{p}^*}{\partial\tilde{r}} + \frac{1}{K_{LR}}\left(\nabla^2\tilde{u} - \frac{\tilde{u}}{\tilde{r}^2} - \frac{2}{\tilde{r}^2}\frac{\partial\tilde{v}}{\partial\theta}\right), \tag{25}$$

$$\tilde{u}\frac{\partial\tilde{v}}{\partial\tilde{r}} + \frac{\tilde{v}}{\tilde{r}}\frac{\partial\tilde{v}}{\partial\theta} + \frac{\tilde{u}\tilde{v}}{\tilde{r}} + 2\tilde{w}\sin\theta = -\frac{1}{\tilde{r}}\frac{\partial\tilde{p}^*}{\partial\theta} + \frac{1}{K_{LR}}\left(\nabla^2\tilde{v} - \frac{\tilde{v}}{\tilde{r}^2} + \frac{2}{\tilde{r}^2}\frac{\partial\tilde{u}}{\partial\theta}\right), \tag{26}$$

$$\tilde{u}\frac{\partial\tilde{w}}{\partial\tilde{r}} + \frac{\tilde{v}}{\tilde{r}}\frac{\partial\tilde{w}}{\partial\theta} + \frac{2}{Ro}(\tilde{u}\cos\theta - \tilde{v}\sin\theta) = \tilde{C}_2 + \frac{1}{K_{LR}}\nabla^2\tilde{w}. \tag{27}$$

It can be seen from the above equations that the two dimensionless parameters corresponding to K_{LC} and λ are $K_{LR} = Re/Ro^{\frac{1}{2}}$ and the Rossby number $Ro = w_m/\Omega d$. K_{LR} is a parameter that was introduced by Ishigaki & Tamura (1990). It is equal to the ratio of the square root of the product of inertia and Coriolis forces to the viscous force. This is the Reynolds number based on U_{SR}. The Rossby number is the ratio of the inertia force to the Coriolis force. If we replace the Coriolis force in K_{LR} and Ro with a centrifugal force, we get K_{LC} and λ.

If we bring Ro to infinity, terms including Ro disappear in (27). The limiting forms of (24)–(27) then do not include Ro and the flow properties of rotating pipe flow are governed only by K_{LR}. The limiting equations for a 'weakly rotating' pipe flow are similar to those for a 'weakly curved' or 'loosely coiled' pipe flow, as shown in (12)–(15), except for body force terms.

The centrifugal force in curved pipe flow is proportional to w^2/R, while the Coriolis force in rotating pipe flow is proportional to Ωw. As these two forces can never be equal everywhere in the cross-section, the analogy described in this paper is not exact but of an approximate nature. The degree of coincidence varies from one flow property to another. We will see that integral properties, such as friction factor and heat transfer rate, show good agreement. Some discrepancy can be seen for local properties like maximum values of primary and secondary velocities.

It is of some use to comment here that $K_{L(tr)}$, values of K_{LC} or K_{LR} where transition to turbulence occurs, does not satisfy the 'asymptotic invariance property'. As $K_{L(tr)}$

should asymptote to $Re = 2320$, the critical value for non-rotating straight pipe flow, when λ or Ro are very large, we have

$$K_{LC} \to 2320/\lambda^{\frac{1}{2}} \quad \text{or} \quad K_{LR} \to 2320/Ro^{\frac{1}{2}} \qquad \text{as} \quad \lambda \quad \text{or} \quad Ro \to \infty.$$

These asymptotic values inevitably include the parameters λ and Ro. Comparison of experimental data for $K_{L(tr)}$ (the lower critical value obtained by imposing highly disturbed conditions at the entry of a pipe), taken from Ito (1959) for curved pipe flow and from Ito & Nanbu (1971) for rotating pipe flow, shows considerable discrepancy between them. Therefore the analogy described here cannot be applied to transition to turbulence.

For rotating pipe flow, we will solve (16)–(19) which include the effects of Ro. In order to know how well the 'asymptotic invariance property' of the second parameter, Ro, is satisfied for each flow property even when Ro is large, we will give two computational results, one for $Ro = 10$ and the other for $Ro = 100$. A single curve will be used in the figures when the two results coincide.

3. Outline of the numerical calculation method

The sets of equations (12)–(15) in dimensional form and (16)–(19) are solved individually under steady conditions. The numerical scheme employed to solve these equations is based on the finite-volume approach, which is an adaptation of that of Patankar (1980). The main features of this method include a staggered mesh system, a power-law formulation for the combined convection–diffusion influence, an equation-solving scheme that consists of a block-correction method coupled with a line-by-line procedure, and a well-known SIMPLE procedure for velocity–pressure linkage.

The computational grid covers only a semicircular sector because the flow must be symmetric with respect to the x-axis. The grid density employed is 32 in the r-direction and 27 in the θ-direction. The grid spacing is nearly uniform in the θ-direction. In the r-direction the grid lines are more closely spaced near the wall than near the centre. The accuracy of the 32×27 grid computation was confirmed by repeating calculations with finer and coarser grids. The convergence criterion was specified with all the normalized residual errors for u, v, w and mass to be less than 10^{-6}.

The boundary conditions for the velocities u, v and w are no-slip conditions on the walls of the pipe:

$$u = v = w = 0 \quad \text{at} \quad r = d/2. \tag{28}$$

The boundary conditions for the plane of symmetry are

$$\frac{\partial u}{\partial \theta} = \frac{\partial w}{\partial \theta} = 0 \quad \text{and} \quad v = 0 \quad \text{at} \quad \theta = 0, \pi. \tag{29}$$

In this formulation pressure specifications on the boundaries are not required. At the centre of the pipe, treatments similar to those of Soh & Berger (1984) and Humphrey, Iacovides & Launder (1985) were used to avoid having too many coincidental nodes, each corresponding to a different circumferential angle, at $r = 0$.

4. Results and discussion

4.1. *Friction factor*

Parameters K_{LC} and K_{LR} are the Reynolds number of each flow based on cross-sectional scales. The calculations compare solutions of the two problems when $K_{LC} = K_{LR}$. Figure 3 shows the computational results for the friction factors of these two

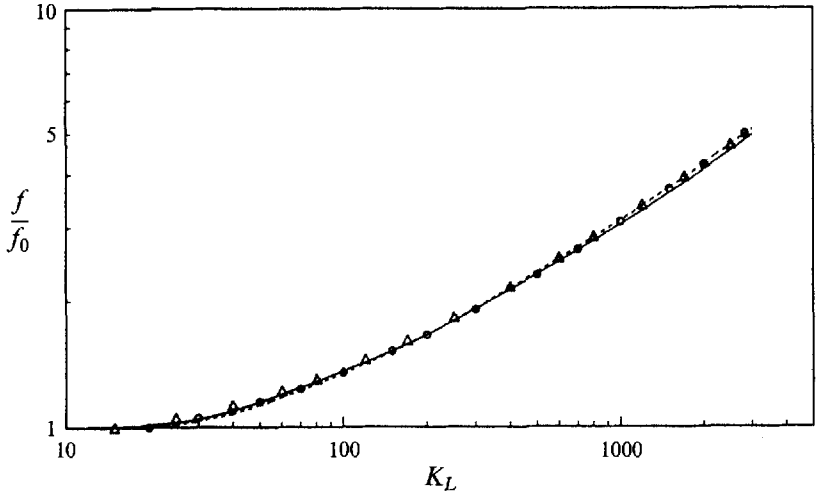

FIGURE 3. Friction factor ratio (f_0: value of a non-rotating straight pipe). Present computations: ——, curved pipe flow; – – –, rotating pipe flow. Experimental data: ○, Ito (curved flow); △, Ito & Nanbu (rotating pipe flow).

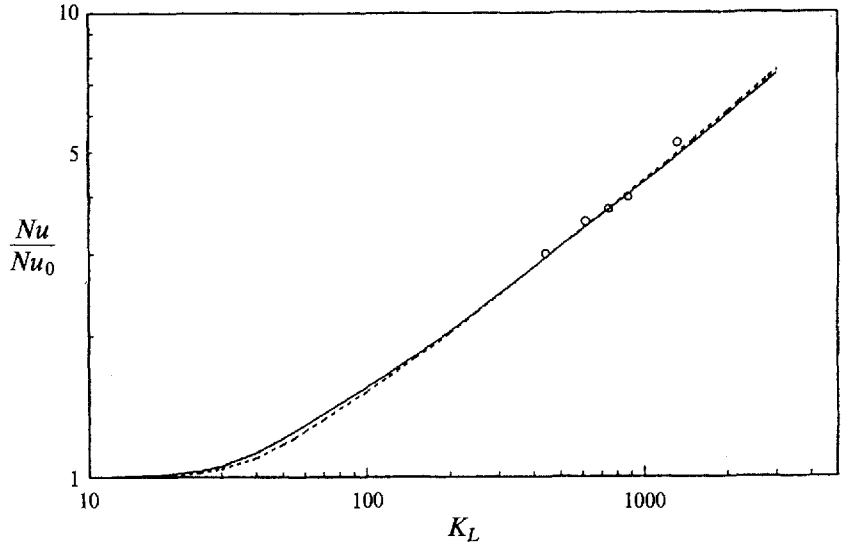

FIGURE 4. Nusselt number ratio for a Prandtl number of 0.71 (Nu_0: value of a non-rotating straight pipe). Present computations: ——, curved pipe flow; – – –, rotating pipe flow. ○, Experimental data by Mori *et al.* for curved pipe flow.

flows, together with experimental data from Ito (1959) for curved pipe flow, and from Ito & Nanbu (1971) for rotating pipe flow. This figure shows that the experimental data coincide. Computational results of the two flows also coincide and agree with the experimental data. As computational results for $Ro = 100$ and 10 coincide, a single curve is shown for rotating pipe flow.

From the above analysis, it is found that the friction factors of these flows can in practice be expressed by a single formula

$$\frac{f}{f_0} = K_L^{\frac{1}{2}}(0.0899 + 1.11K_L^{-0.701}), \tag{30}$$

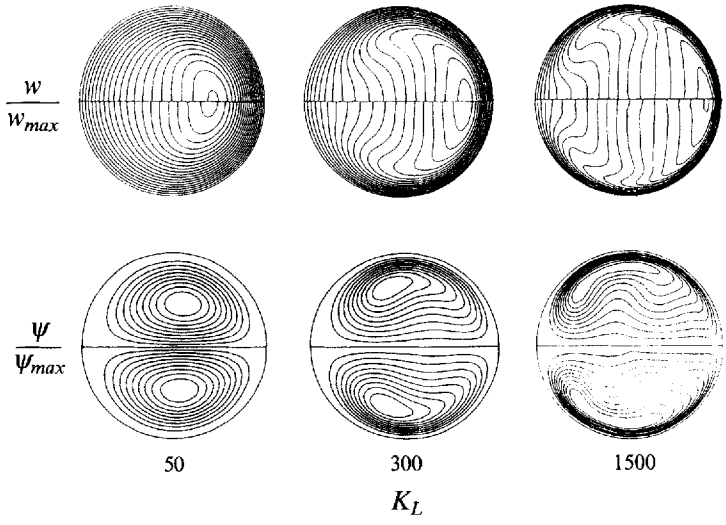

FIGURE 5. Contours of axial velocity and secondary stream functions (upper half: curved pipe flow, lower half: rotating pipe flow).

for $15 < K_L < 3000$, and λ, $Ro > 8$. Here $f_0 = 64/Re$ is the friction factor for non-rotating straight pipe flow while K_L represents K_{LC} for curved pipe flow, and K_{LR} for an orthogonally rotating pipe flow.

4.2. *Heat transfer rate*

Although the heat transfer problem is excluded from the present argument on similarity, we can assume, nevertheless, that this analogy is valid for it too. We will therefore give an example of the heat transfer rate. Figure 4 shows the mean Nusselt number ratio with a Prandtl number of 0.71, which includes computational results for curved pipe flow and rotating pipe flow as well as experimental data by Mori & Nakayama (1967) for curved pipe flow. The thermal boundary condition is an axially constant heat flux at the wall with a peripherally uniform wall temperature. The results for these two flows coincide.

4.3. *Flow patterns*

For the same three values of K_{LC} and K_{LR}, figure 5 shows computational contours for non-dimensional axial velocity and a secondary streamline. The upper half of the pipe cross-section shows curved pipe flow while the lower half shows rotating pipe flow. For all three values of K_L, the contours of the two flows are very similar, particularly for secondary streamlines.

4.4. *Other flow properties*

When λ and Ro are large enough, the location of the maximum axial velocity w_{max} shifts on the x-axis from the centre of the pipe to the pressure side, as K_L increases. Figure 6 shows a variation of w_{max}/w_m with K_L. For a moderate K_L the two values are the same, but they differ when $K_L \approx 150$. The asymptotic values are somewhat different, but the overall behaviour is similar. When comparing the calculations for $Ro = 10$ and 100 in rotating pipe flow, the maximum axial velocity seems to be somewhat influenced by Ro, even if Ro is greater than 10.

If we take the wall values at $\theta = 180°$ as a reference pressure, the contours of the cross-sectional pressure for each flow, p and p^*, are lines roughly parallel to the y-axis.

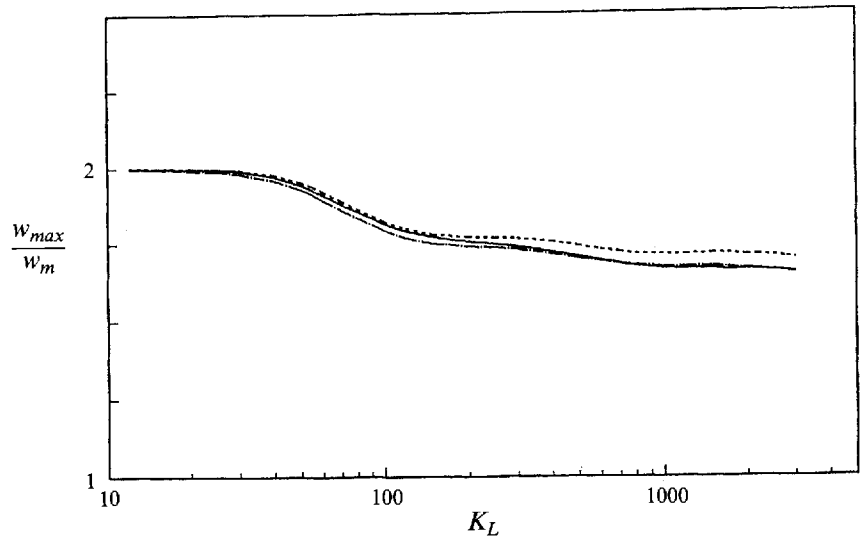

FIGURE 6. Variation of the maximum axial velocity with K_L: ——, curved pipe flow; – – –, rotating pipe flow ($Ro = 100$); —·—, rotating pipe flow ($Ro = 10$).

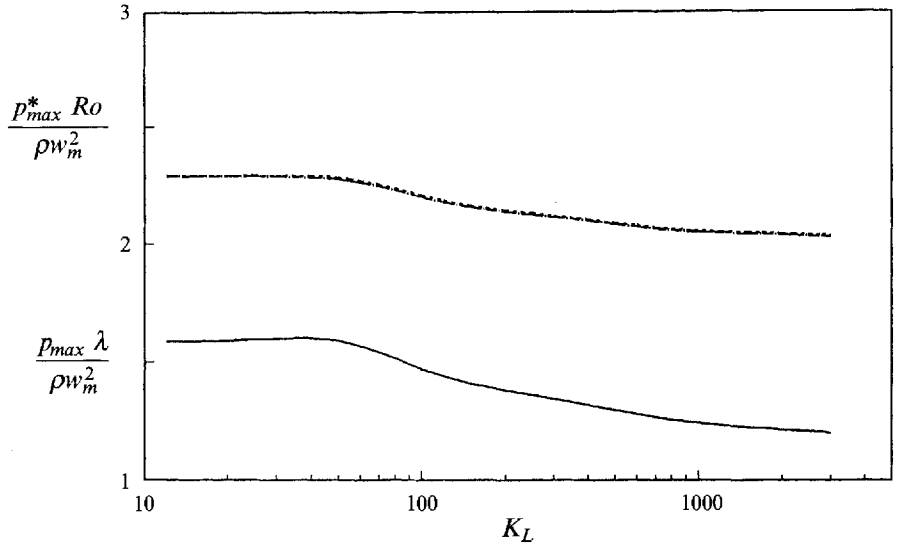

FIGURE 7. Variation of the maximum cross-sectional pressure difference with K_L: ——, curved pipe flow; – – –, rotating pipe flow ($Ro = 100$); —·—, rotating pipe flow ($Ro = 10$).

The maximum pressure difference, p_{max} or p^*_{max}, is the wall pressure difference between $\theta = 0°$ and 180°. These are normalized using (7) and (23). Variations of $\tilde{p}_{max}$ and $\tilde{p}^*_{max}$ with K_L are shown in figure 7. These are essentially different, since p^* is the reduced pressure defined by (20). In spite of this, the variations of $\tilde{p}_{max}$ and $\tilde{p}^*_{max}$ with K_L are quite similar.

The secondary stream function maximum ψ_{max} is located at the centre of secondary flow vortices as shown in figure 5. Variations of ψ_{max}, normalized using (7) and (23), with K_L are shown in figure 8. The secondary flow velocity $V_S = (u^2 + v^2)^{\frac{1}{2}}$ reaches its

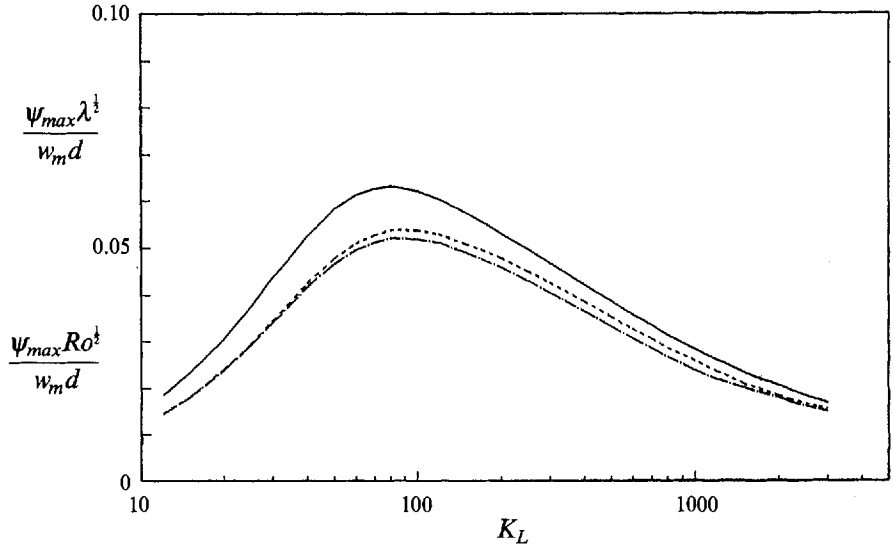

FIGURE 8. Variation of the stream function maximum ψ_{max} with K_L: ——, curved pipe flow; – – – –, rotating pipe flow ($Ro = 100$); —·—, rotating pipe flow ($Ro = 10$).

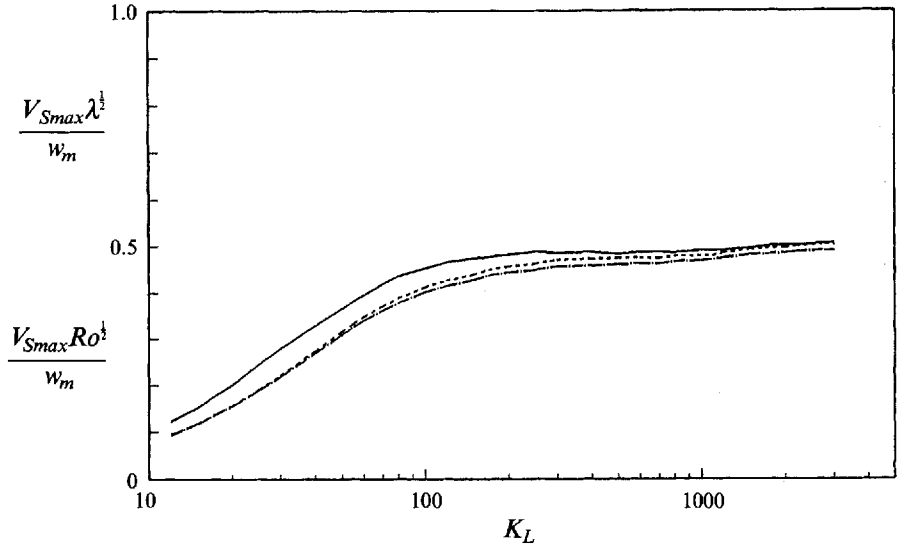

FIGURE 9. Variation of the maximum secondary velocity with K_L: ——, curved pipe flow; – – – –, rotating pipe flow ($Ro = 100$); —·—, rotating pipe flow ($Ro = 10$).

maximum near the wall around $\theta = 90°$. A variation of the normalized maximum value V_{Smax} with K_L is shown in figure 9. These two figures also show similar quantitative behaviour in secondary flow properties.

The quantitative correspondence to these local properties between the two flows are not as good as those of integral properties like friction factor and heat transfer rate. The discrepancy of local properties comes from the local difference between the centrifugal force and the Coriolis force. Nevertheless, variations of local properties with K_{LC} or K_{LR} are quite similar and the relative differences are within 16%, except for figure 7.

5. Conclusions

A quantitative analogy between fully developed laminar flows in curved pipes and in orthogonally rotating pipes has been demonstrated using similarity arguments and computational studies. The new dimensionless parameter K_{LR} was introduced for rotating pipe flow where a set of K_{LR} and the Rossby number Ro were found to correspond with a set of the Dean number K_{LC} and the curvature ratio λ in curved pipe flow. When λ and Ro were large enough, K_{LC} and K_{LR} became the sole governing parameters in their respective flows, so the analogy between the two flows became evident. Through experimental data and computational results it was demonstrated that the friction factor, and heat transfer rate, of the two flows coincided. Primary and the secondary cross-sectional flow patterns were proven to be similar for a wide range of parameters. Flow variables, such as the maximum axial velocity and secondary velocity of the two flows, exhibited similar behaivour when they were normalized according to the proper scaling method.

This analysis does not carry over to turbulent flows. An analysis on turbulent flows will be made separately.

REFERENCES

Akiyama, M. & Cheng, K. C. 1971 Boundary vorticity method for laminar forced convection heat transfer in curved pipes. *Intl J. Heat Mass Transfer* **14**, 1659.

Austin, L. R. & Seader, J. D. 1973 Fully developed viscous flow in coiled circular pipes. *AIChE J.* **19**, 85.

Barua, S. N. 1954 Secondary flow in a rotating straight pipe. *Proc. R. Soc. Lond.* A **227**, 133.

Benton, G. S. & Boyer, D. 1966 Flow through a rapidly rotating conduit of arbitrary cross-section. *J. Fluid Mech.* **26**, 69.

Berger, S. A., Talbot, L. & Yao, L. S. 1983 Flow in curved pipes. *Ann. Rev. Fluid Mech.* **15**, 461.

Collins, W. M. & Dennis, S. C. R. 1975 The steady motion of a viscous fluid in a curved tube. *Q. J. Mech. Appl. Maths* **28**, 133.

Dean, W. R. 1927 Note on the motion of fluid in a curved pipe. *Phil. Mag.* **4**, 208.

Dean, W. R. 1928 The streamline motion of fluid in a curved pipe. *Phil. Mag.* **5**, 673.

Dennis, S. C. R. & Ng, M. 1981 Dual solutions for steady laminar flow through a curved tube. *Q. J. Mech. Appl. Maths* **35**, 305.

Humphrey, J. A. C., Iacovides, H. & Launder, B. E. 1985 Some numerical experiments on developing laminar flow in circular-sectioned bends. *J. Fluid Mech.* **113**, 357.

Ishigaki, H. & Tamura, H. 1990 Fluid flow and heat transfer in orthogonally rotating pipes. In *3rd Japan–China Joint Conf. on Fluid Machinery*, vol. 2, p. 267. Japan Soc. Mech. Engrs.

Ito, H. 1959 Friction factors for turbulent flow in curved pipes. *Trans. ASME* D: *J. Basic Engng* **81**, 123.

Ito, H. 1987 Flow in curved pipes. *Japan Soc. Mech. Engng Intl J.* **30**, 543.

Ito, H., Hasegawa, S. & Yano, M. 1986 Numerical calculations of laminar flow in rotating pipes. *Rep. Inst. High Speed Mech., Tohoku-University* **56**, 75 (in Japanese).

Ito, H. & Nanbu, K. 1971 Flow in rotating straight pipes of circular cross section. *Trans. ASME* D: *J. Basic Engng* **93**, 383.

Kheshgi, H. S. & Scriven, L. E. 1985 Viscous flow through a rotating square channel. *Phys. Fluids* **28**, 2968.

Komiyama, Y., Mikami, F. & Okui, K. 1986 Laminar forced convection heat transfer in rectangular ducts rotating about an axis perpendicular to the duct axis. *Trans. Japan Soc. Mech. Engng* **52-B**, 3761 (in Japanese).

Lei, U. & Hsu, C. H. 1989 Flow through rotating straight pipes. *Phys. Fluids* A **2**, 63.

McConalogue, D. J. & Srivastava, R. S. 1968 Motion of fluid in a curved tube. *Proc. R. Soc. Lond.* A **307**, 37.

MORI, Y. & NAKAYAMA, W. 1967 Study on forced convective heat transfer in curved pipes (1st report, laminar region). *Intl J. Heat Mass Transfer* **8**, 67.

MORI, Y. & NAKAYAMA, W. 1968 Convective heat transfer in rotating radial circular pipes (1st report, laminar region). *Intl J. Heat Mass Transfer* **11**, 1027.

MORRIS, W. D. 1981 *Heat Transfer and Fluid Flow in Rotating Coolant Channels*. Research Studies Press.

NANDAKUMAR, K. & MASLIYAH, J. H. 1982 Bifurcation in steady laminar flow through curved tubes. *J. Fluid Mech.* **119**, 475.

NANDAKUMAR, K. & MASLIYAH, J. H. 1986 Swirling flow and heat transfer in coiled and twisted pipes. In *Advances in Transport Processes* (ed. A. S. Mujumdar & R. A. Mashelkar), vol. 4, p. 49. J. Wiley.

PATANKAR, S. V. 1980 *Numerical Heat Transfer and Fluid Flow*. Hemisphere.

PATANKAR, S. V., PRATAP, V. S. & SPALDING, D. B. 1974 Prediction of laminar flow and heat transfer in helically coiled pipes. *J. Fluid Mech.* **62**, 539.

SKIADARESSIS, D. & SPALDING, D. B. 1977 Heat transfer in a pipe rotating around a perpendicular axis. *Imperial College Heat Transfer Section Rep.* HTS/77/3.

SOH, W. Y. & BERGER, S. A. 1984 Laminar entrance flow in a curved pipe. *J. Fluid Mech.* **148**, 109.

SOH, W. Y. & BERGER, S. A. 1987 Fully developed flow in a curved pipe of arbitrary curvature ratio. *Intl J. Numer. Meth. Fluids* **7**, 733.

SPEZIALE, C. G. 1982 Numerical study of viscous flow in rotating rectangular ducts. *J. Fluid Mech.* **122**, 251.

THANGAM, S. & HUR, N. 1990 Laminar secondary flows in curved rectangular ducts. *J. Fluid Mech.* **217**, 421.

TRUESDELL, L. C. & ADLER, R. J. 1970 Numerical treatment of fully developed laminar flow in helically coiled tubes. *AIChE J.* **16**, 1010.

WARD-SMITH, A. J. 1980 *Internal Fluid Flow*, p. 251. Clarendon.